# Nature of the magnetoelectric coupling in multiferroic $Pb(Fe_{1/2}Nb_{1/2})O_3$ ceramics

M. H. Lente,* J. D. S. Guerra, G. K. S. de Souza, B. M. Fraygola, C. F. V. Raigoza, D. Garcia, and J. A. Eiras
*Grupo de Cerâmicas Ferroelétricas, Departamento de Física, Universidade Federal de São Carlos, CEP 13565-670 São Carlos, São Paulo, Brazil*

(Received 28 November 2007; revised manuscript received 30 May 2008; published 12 August 2008)

In this work, electrical permittivity measurements in lead iron niobate (PFN) ceramics were performed in the frequency and temperature ranges from 10 kHz to 1.2 GHz and from 15 to 450 K, respectively. The microwave dielectric results characterized unambiguously the magnetoelectric effect in PFN and demonstrated that the nature of such coupling arises indirectly via ferroelastic contribution rather than a direct coupling between electrical and magnetic order parameters. Moreover, it was also verified that such coupling can be enhanced or suppressed depending on the relative orientation between the probing electric field and the macroscopic ferroelectric polarization.

DOI: 10.1103/PhysRevB.78.054109 PACS number(s): 77.84.Dy, 77.22.Jp, 77.80.Bh

## I. INTRODUCTION

From the fundamental point of view, magnetoelectric materials present coupled magnetic and electrical order parameters and such magnetoelectric coupling can exist whatever the nature of magnetic and electrical order parameters is.[1–3] Of particular interest is single-phase magnetoelectric multiferroic materials, in which all the three ferroic properties can coexist and are intrinsically coupled: ferroelectricity, ferromagnetism, and ferroelasticity.[1,4,5] Nowadays the term *multiferroic* includes materials that have antiferroic orders.[1] Furthermore, the ferroic nomenclature has been enlarged with subdivision into primary, secondary, and tertiary ferroics, which naturally include the magnetoelectric multiferroic materials.[6,7]

The nub of such ferroic systems is the existence of distinct coupled switchable domain states,[8–10] which can be driven by one specific ferroic driving force or a combination of these.[11] Consequently, the macroscopic properties of magnetoelectric multiferroic materials are determined by the relation among the respective domain states, which exhibit different tensor components of the magnetoelectric tensor.[12,13] Therefore, due to the distinct but coupled domain states feature, it is expected that a change in just one ferroic domain state can modify at least one component of magnetoelectric tensor, thus modifying the macroscopic magnetoelectric coupling components of a multiferroic material.

Regarding the coupling between the order parameters, it has been proposed that in single-phase multiferroic systems, the magnetoelectric coupling may arise directly between electrical and magnetic order parameters or indirectly via lattice strain.[1,3,14,15] The last mechanism is technologically more interesting because it often enhances the magnetoelectric coupling by several orders of magnitude, as observed in some composites.[16–18] However, although the effects of ferroelasticity on the magnetoelectric coupling may be significant or even dominant, they have been rarely included in the Landau theory in writing the free energy of the magnetoelectric multiferroic systems, probably due to the lack of experimental knowledge about their effective contribution to the magnetoelectric coupling. Indeed, usually only the magnetic (**M**) and electrical (**P**) contributions have been taken into account.[3] Then, a thermodynamic potential including also the spontaneous strain ($\varepsilon$) and stress ($\sigma$) that applies for all orientation states may be written as[19]

$$G_{(M,P,\sigma)} = \varepsilon_{ij}\sigma_{ij} + P_iE_i + M_iH_i + \frac{1}{2}s_{ijkl}\sigma_{ij}\sigma_{kl} + \frac{1}{2}\kappa_{ij}E_iE_j + \frac{1}{2}\chi_{ij}H_iH_j + d_{ijk}E_i\sigma_{jk} + Q_{ijk}H_i\sigma_{jk} + \alpha_{ij}H_iE_j + \cdots, \quad (1)$$

where $s_{ijkl}$, $\kappa_{ij}$, and $\chi_{ij}$ are, respectively, the elastic compliance, electric susceptibility, and magnetic susceptibility tensors. $d_{ijk}$ and $Q_{ijk}$ describe the piezoelectric and the piezomagnetic tensors, respectively, while $\alpha_{ij}$ represents the linear magnetoelectric coefficient. Naturally higher-order coefficients may be considered but with the free energy expanded to higher-order terms. A wide variety of ferroic phenomena is possible, depending on which terms in $G(M,P,\sigma)$ are important.

The most usual method for probing the magnetoelectric coupling consists of determining changes either in the magnetization through the ferroelectric phase transition or, conversely, in the electrical permittivity through a magnetic ordering.[1,20,21] However, these conventional measurements do not provide enough information about the coupling mechanism or the influence of the elastic contribution on such coupling.[1,21] In this context, microwave dielectric spectroscopy has been revealed as a powerful tool for probing structural phase transitions[22,23] and dynamical changes in domain and nanodomain structures.[22,24,25] Moreover, this technique has been also revealed to be very selective for identifying and even for separating the ferroelastic contribution to the dielectric response of ferroelectric-ferroelastic multiferroic materials.[22,26] Therefore, microwave dielectric spectroscopy could be used as an accurate approach to investigate the ferroelastic contributions in multiferroic materials, including naturally the magnetoelectric ones.

Lead iron niobate (PFN) remains a promising single-phase multiferroic material that has been largely investigated due to its structural simplicity and, thus, may be considered a prototype material.[27–29] There is a consensus that PFN under-

 

goes a paraelectric-to-ferroelectric phase transition near 376 K (Refs. 30–32) and a paramagnetic-to-antiferromagnetic ordering at the Néel temperature $T_N \approx 143$ K,[33,34] in which a magnetoelectric coupling between the ferroelectric and antiferromagnetic orders occurs. However, although the ferroelectric and antiferromagnetic properties of PFN are well established,[33–35] the magnetoelectric effect has been scarcely investigated. Consequently, the exact nature of the magnetoelectric coupling effect in the PFN remains still open; thus it is a subject of continuing debate, as reviewed recently in some works.[36,37]

The aim of this work is threefold: first, to characterize unambiguously through microwave dielectric measurements the magnetoelectric effect in multiferroic PFN ceramics; second, to determine the nature of such magnetoelectric coupling; and finally, to investigate how a change in a ferroic domain state modifies the magnetoelectric coupling in PFN.

## II. EXPERIMENTAL PROCEDURE

High quality $[Pb(Fe_{1/2}Nb_{1/2})O_3]$ (PFN) ceramics were synthesized by using the *B*-site precursor route and sintered by uniaxial hot-pressing method. Briefly, the monoclinic $FeNbO_4$ precursor was synthesized by solid-state reaction of reagent grade iron oxide, $Fe_2O_3$ (Aldrich, 99.9%), and niobium oxide, $Nb_2O_5$ (Aldrich, 99.9%), in accordance to the route proposed by some authors.[38] The precursor oxides were weighed according to the desired stoichiometry and after that were mixed for 4 h in a ball mill using distilled water as solvent and stabilized $ZrO_2$ balls as grinding medium. The calcining temperature chosen for the monoclinic phase was 1323 K, as proposed in the literature.[38,39] Then, the $FeNbO_4$ and PbO powders (NGK, 99.3%) were stoichiometrically mixed in ball mill using distilled water, dried, and then calcined at 1073 K to form PFN. Hot-pressed PFN pellets were sintered at 1300 K for 3 h under a uniaxial pressure of 5 MPa in controlled oxygen atmosphere.

The relative densities of sintered samples were determined by the Archimedes method, while their morphological features were analyzed in a Jeol 5800LV scanning electron microscope (SEM). The x-ray powder diffraction patterns were measured at room temperature on a Rigaku Denki powder diffractometer with geometry $\theta-2\theta$, rotating anode x-ray source (Cu $K\alpha$ radiation, $\lambda = 1.542$ Å), and scintillation detector.

The sintered ceramic bodies were cut into bars and polished to a thickness of 0.5 mm for dielectric measurements. After that, they were annealed at 900 K for 0.5 h to release mechanical stresses introduced during the polishing, and then gold electrodes were sputtered onto the sample surfaces. In particular, one sample was poled under an electric field of 15 kV/cm for 30 min at room temperature. This poled sample was then carefully cut into two pieces. While in one piece the microwave dielectric properties were characterized parallel ($\parallel$) to the poling direction (labeled as $P_3$), in the other one these were characterized perpendicularly ($\perp$), as described in a previous work.[26] The purpose of this poling procedure in the PFN ceramic was to produce a macroscopic ferroelectric-ferroelastic domain orientation in order to enable us to investigate the effective contribution of the elastic component to the magnetoelectric coupling.

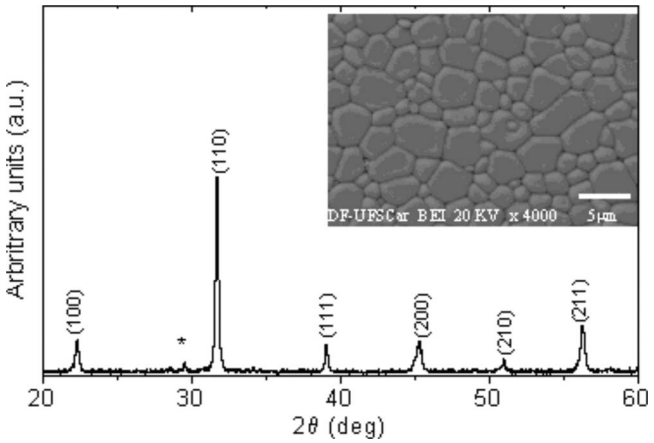


FIG. 1. X-ray diffraction patterns of sintered PFN samples. The inset shows the surface microstructure of PFN sample. * represents $Pb_2Nb_2O_7$.

The microwave dielectric measurements were carried out in the temperature range of 80–300 K using a HP 8719C network analyzer (Refs. 25 and 26) in an unpoled sample and in both poled samples (parallel and perpendicular to the poling direction). Low-frequency measurements were performed in the unpoled sample using an HP 4194A impedance analyzer from 15 to 450 K at a constant cooling rate of 2 K/min. It must be highlighted that the true magnetoelectric coupling should be preferentially investigated at high frequencies to suppress the contribution of charge carries, present usually at low frequencies.[21]

## III. RESULTS AND DISCUSSION

The microstructural analysis of PFN samples revealed a uniform microstructure with an average grain size of 3.9 $\mu$m and a density higher than 98% of the ideal one. In addition, x-ray diffraction (XRD) measurements of the sintered samples revealed a very good crystallization of PFN single phase with a pseudocubic structure, which is in accordance to the literature.[27,39] These results are shown in Fig. 1.

Figure 2(a) shows the temperature and frequency dependence of the real ($\varepsilon'$) and imaginary ($\varepsilon''$) components of the relative dielectric permittivity of the unpoled PFN ceramic measured in the radio frequency range. The electrical permittivity curve shows a clear maximum (peak) at $\approx$379 K, which can be straightly associated with the paraelectric-ferroelectric phase transition ($T_C$), as confirmed by structural analysis.[31,32]

Figure 2(b) depicts the electrical permittivity measured at low temperatures. These data reveal a broad shoulder from $\approx$300 to 100 K, which is visualized only in the imaginary component of the electrical permittivity ($\varepsilon''$). In a previous work, an identical behavior was found in both ordinary and relaxor ferroelectric perovskite compounds.[40] This phenomenon seems to be very common in multiferroic systems whatever the nature of order parameter is. Thus it demands further investigation that is beyond the scope of this work.

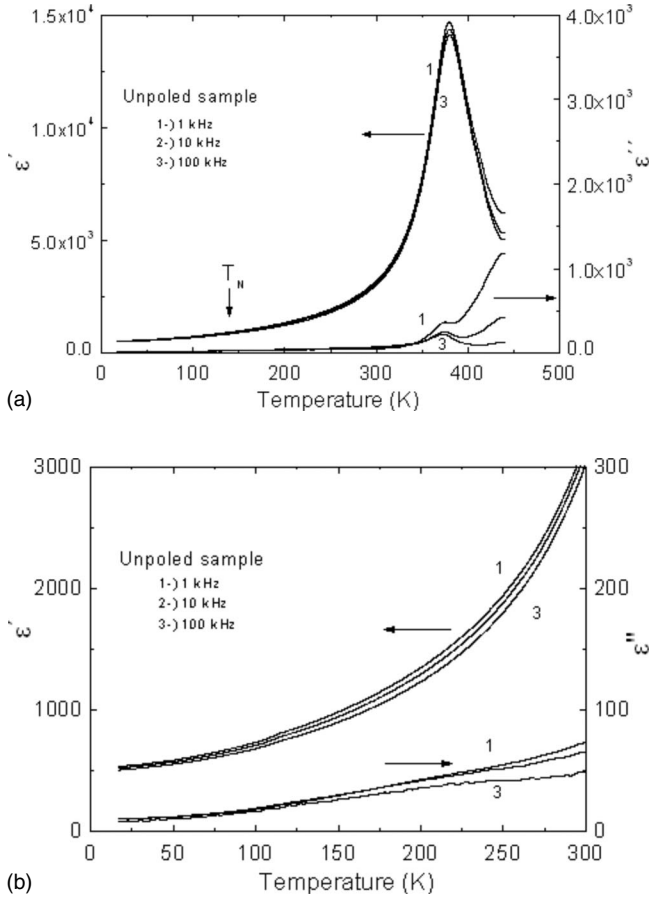


FIG. 2. (a) Temperature and frequency dependence of the real ($\varepsilon'$) and imaginary ($\varepsilon''$) components of the relative dielectric permittivity of PFN ceramics measured in the radio frequency range; (b) frequency dependence of $\varepsilon'$ and $\varepsilon''$ for the PFN ceramic measured down from 300 to 15 K.

Therefore, in the face of its apparent universality and its broadband characteristic, the dielectric anomaly bellow 300 K cannot be necessarily associated with the magnetoelectric coupling. Rather, dielectric anomalies in PFN ceramics characterized around the Néel temperature and in the radio frequency range are usually very subtle. They are better observed only in single crystals.[37,41] This fact may be related to one of the limitations of radio frequency dielectric measurements to detect weak phase transitions in bulk ceramics.[42]

Figures 3(a) and 3(b) depict representative curves of the frequency dependence of the real ($\varepsilon'$) and imaginary ($\varepsilon''$) parts of the relative dielectric permittivity measured in the microwave range in the unpoled PFN sample. Similar curves were also obtained for the poled samples measured perpendicular and parallel to the poling direction. The data reveal strong temperature dependent dielectric dispersions in the gigahertz range, which is characterized by a decrease in $\varepsilon'$ and a maximum (peak) in $\varepsilon''$ with increasing the frequency. This feature is typical of ferroelastic-ferroelectric ferroic materials and can be described as a damped or overdamped resonance process rather than a simple Debye dielectric relaxation.[26]

From the dielectric dispersion curves (Fig. 3), the characteristic frequency ($f_R$) and the dielectric strength ($\Delta\varepsilon$) were

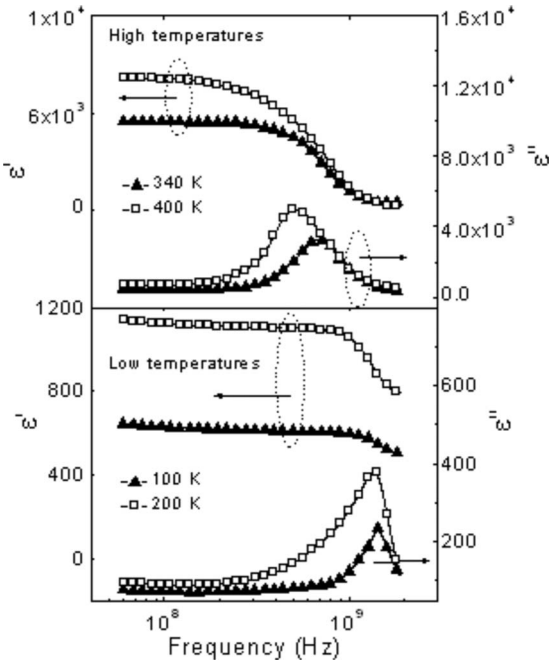


FIG. 3. Representative curves of the real ($\varepsilon'$) and imaginary ($\varepsilon''$) parts of the relative dielectric permittivity for PFN ceramics as a function of the temperature and frequency in the microwave range.

determined. The dielectric strength is defined as $\Delta\varepsilon=\varepsilon_0-\varepsilon_\infty$, while the characteristic frequency is the frequency at the maximum of the imaginary component of dielectric constant ($\varepsilon''$).[43] The procedure used to determine $\Delta\varepsilon$ and $f_R$ from the PFN data are schematically illustrated in Figs. 4(a) and 4(b), respectively.

Figure 5 shows the temperature dependence of the characteristic frequency ($f_R$) and the dielectric strength ($\Delta\varepsilon$) for the unpoled and poled [parallel ($\parallel$) and perpendicular ($\perp$) to the poling direction] PFN samples. In contrast to the radio frequency dielectric measurements (Fig. 2), the data obtained from the microwave measurements revealed for the unpoled sample clear dielectric anomalies (a peak in $\Delta\varepsilon$ and a local minimum for $f_R$) around $T\approx 149$ K. This temperature coincides very well with the temperature reported for the paramagnetic-antiferromagnetic ordering ($T_N\approx 143$ K).[33,34,36,37] Therefore, unless another unknown ordering superimposed over the magnetic ordering, this dielectric anomaly is caused by the magnetoelectric coupling in the PFN system. This result demonstrates the high sensitivity of microwave dielectric measurements to probe weak transitions in bulk ceramics, as proposed before.[42]

Concerning now the nature of such magnetoelectric coupling, in relation to the unpoled sample it is verified that $f_R$ and $\Delta\varepsilon$ characterized parallel and perpendicular to the poling direction present remarkable distinct behaviors. Indeed, Fig. 5 shows that the anomalies in $f_R$ and $\Delta\varepsilon$ curves around the Néel temperature ($T_N\approx 149$ K) are strongly enhanced when the dielectric measurement is performed $\parallel$ to the poling direction. In contrast, they are practically suppressed when the sample is characterized $\perp$ to the poling direction. Therefore, in relation to the poled PFN sample, these results reveal that

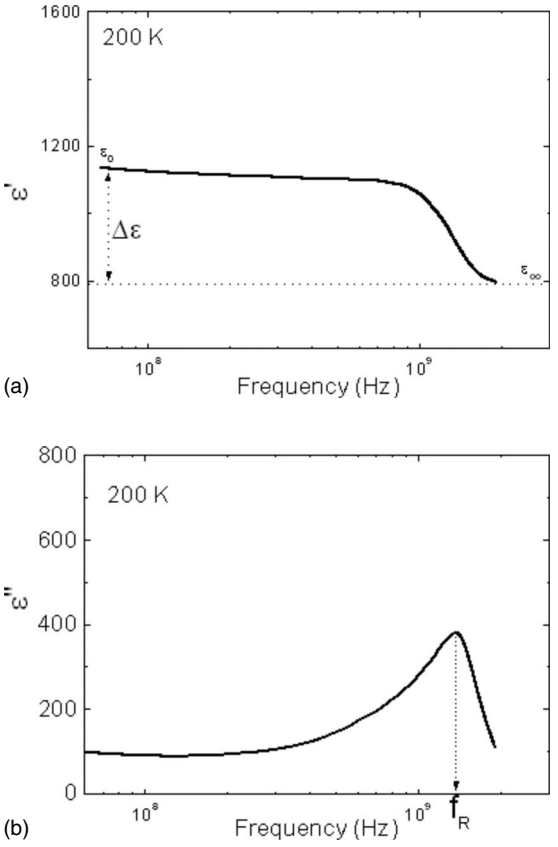


FIG. 4. Definition and experimental procedure used to determine the dielectric strength ($\Delta\varepsilon$) and the characteristic frequency ($f_R$) from the real and imaginary components of dielectric constant. The curves shown were measured at 200 K.

the magnetoelectric coupling is highly anisotropic and such coupling can be enhanced or suppressed depending on the relative orientation between the probing electric field and the macroscopic polarization.

As discussed in Sec. I, we poled the as fired PFN ceramic to switch the original ferroelectric domain state. Then, by

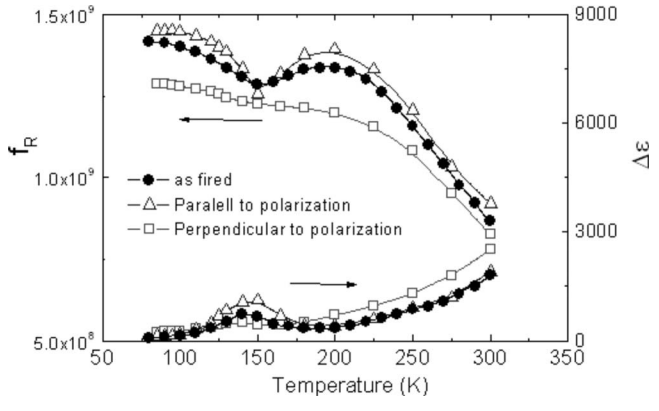


FIG. 5. Temperature dependence of the characteristic frequency ($f_R$) and dielectric strength ($\Delta\varepsilon$) for the unpoled and poled PFN ceramics. The symbol (●) represents the data for the unpoled sample, while (Δ) and (□) represent the data for the poled PFN ceramics measured parallel (∥) and perpendicular (⊥) to the poling direction, respectively.

assuming that the all three ferroic domains are mutually coupled, this poling process modifies not only the ferroelectric domain state but the antiferromagnetic and ferroelastic ones as well. Moreover, the poling changes the macroscopic crystallographic symmetry of the ceramic body from $\infty\infty m$ to $6mm$, which in turn, can modify the magnetoelectric response. Thus, it is reasonable to suppose that the magnetoelectric matrix of the poled PFN sample may have components that vanishes ($\alpha_{ij}=0$) or have an arbitrary value ($\alpha_{ij}\neq 0$).[1,13] This fact implies that for that direction in which the magnetoelectric tensor does not vanish ($\alpha_{ij}\neq 0$), the magnetoelectric coupling must be detected in the dielectric measurements. Naturally, for that direction in which the magnetoelectric tensor vanishes ($\alpha_{ij}=0$), the coupling will not be detected. In other words, due to the anisotropy of the magnetoelectric tensors for the PFN poled samples, some degree of anisotropy is expected in the dielectric measurements, as observed in Fig. 5. The fundamental question now is to determine if the magnetoelectric coupling arises directly between the electric and magnetic order parameters or indirectly via strain.

Information about the elastic contribution to the magnetoelectric coupling can be extracted from the dielectric dispersion curves of the poled samples (Figs. 3 and 5) by taking into account the piezoelectric effect. Indeed, since piezoelectricity provides a coupling between elastic and dielectric properties, the piezoelectric properties cannot be discussed without reference to dielectric and elastic constants. Therefore, in order to determine the nature of the magnetoelectric coupling in the PFN ceramic, the dielectric data are now analyzed considering a probing field parallel or perpendicular to the poling direction.

In view of the symmetry of the poled samples ($6mm$) and considering the respective symmetry operations, the piezoelectric effect can be represented by the following equations:[44]

$$\sigma_1 = c_{11}\varepsilon_1 + c_{12}\varepsilon_2 + c_{13}\varepsilon_3 + e_{31}E_3, \tag{2}$$

$$\sigma_2 = c_{12}\varepsilon_1 + c_{11}\varepsilon_2 + c_{13}\varepsilon_3 + e_{31}E_3, \tag{3}$$

$$\sigma_3 = c_{13}\varepsilon_1 + c_{13}\varepsilon_2 + c_{33}\varepsilon_3 + e_{33}E_3, \tag{4}$$

$$\sigma_5 = c_{55}\varepsilon_5 + e_{15}E_1, \tag{5}$$

where $c$ and $e$ are the elastic stiffness and the piezoelectric coefficients, respectively. $E_1$ and $E_3$ are the probing electric fields applied parallel and perpendicular to the poling direction, respectively.

Some important aspects of the piezoelectric equations [Eqs. (2)–(5)] must be highlighted. First, when a probing electric field ($E_3$) is applied parallel to the poling direction ($P_3$), it generates only compressional/extensional stress ($\sigma_1$, $\sigma_2$, or $\sigma_3$). In contrast, when an electric field ($E_1$) is applied perpendicular to poling direction, only shear stress ($\sigma_5$) is generated.[44] The fundamental difference between both cases is that stress generated by the electric field $E_3$ produces volumetric changes in the sample, while fields applied perpendicularly does not ($E_1 \perp P_3$).[45] In other words, ferroelastic dipoles are modified only by the application of an electric

probing field $E_3$, which is parallel to the macroscopic polarization.[44]

This fact has a strong impact on the understanding of magnetoelectric coupling in the PFN. Indeed, since the dielectric anomaly around $T_N$ is enhanced or suppressed when the microwave dielectric properties are measured parallel $(E_3 \| P_3)$ or perpendicular $(E_1 \perp P_3)$ to the poling direction, respectively, the piezoelectric equations show that the higher the ferroelastic contribution is, the higher is the magnetoelectric coupling. Rather, our results reveal that for poled PFN ceramics the magnetoelectric coupling is remarkably enhanced when a compressional/extensional piezoelectric stress is generated $(\sigma_3)$, which in turn is the only stress that interacts with the ferroelastic dipoles.[26,44] In contrast, when the probing field is applied perpendicular to the macroscopic polarization $(E_1 \perp P_3)$, only shear stress $(\sigma_5)$ is generated,[26,44] which does not interact with the ferroelastic dipoles,[45] and consequently, no magnetoelectric coupling is detected (Fig. 5). Therefore, these results reveal clearly that the magnetoelectric coupling in the PFN ceramics arises indirectly via ferroelastic contribution rather than a direct coupling between the electrical and magnetic order parameters.

Our results show that the ferroelastic term must be taken into account either explicitly or implicitly in the free energy of magnetoelectric multiferroic materials for their realistic description. Then by considering the elastic polarization (spontaneous strain) as a primary order parameter, cross terms involving the product of strain and magnetic and electric fields will appear naturally in describing the magnetoelectric coupling. On the other hand, by assuming that the elastic dipole is a secondary order parameter, the magnetoelectric coefficient $(\alpha_{ij})$ would include implicitly the ferroelastic effect. In this case we will have an effective coefficient ($\alpha$ is ferroelastic dependent).

Anisotropic behavior of the dielectric permittivity measured in the radio frequency range has been observed in $MnF_2$ magnetoelectric single crystals near the Néel temperature.[46,47] Such anisotropy was explained in terms of the exchange-striction mechanism coupled to the lattice polarizability via piezoelectric compliances.[46,48] This hypothesis is corroborated by anisotropic crystal lattice distortion presented by the $MnF_2$ accompanying its magnetic ordering.[49] Recently, Rietveld refinements revealed that the lattice parameters of PFN show subtle anisotropic anomalies at the Néel temperature.[50] Therefore, in analogy to the $MnF_2$ case, this fact reinforces our supposition that the magnetoelectric coupling in PFN is strain mediated. However, by using the piezoelectric concepts for poled samples, it is much more rigorous and convincing that the magnetoelectric coupling in PFN is mediated mainly due to ferroelastic contribution and effectively coupled to the electric polarization via piezoelectric compliances.

Finally, let us to return to the fact that the magnetoelectric coupling was observed only in the microwave dielectric measurements (Figs. 2 and 5). While the microwave dielectric properties are directly related to the elastic properties of the lattice,[51,52] the dielectric permittivity measured in the radio frequency range includes several mechanisms,[43] inclusive resistive artifacts (leakage) present at low frequencies that can mask the dielectric measurements.[21] Therefore, this fact associated with the lattice parameter anomalies observed near the Néel temperature in the PFN (Ref. 50) may explain why only the microwave dielectric measurements could detect the magnetoelectric coupling.

## IV. CONCLUSION

In summary, the magnetoelectric effect in multiferroic PFN ceramics was investigated through microwave dielectric measurements. The experimental data revealed that the mechanism responsible for the magnetoelectric effect in the PFN takes place indirectly via ferroelastic contribution rather than a direct coupling between the magnetic and electric order parameters and such coupling depends on the relative orientation between the probing electric field and the macroscopic polarization.

## ACKNOWLEDGMENTS

The authors thank CNPq and FAPESP for the financial support.

*Present address: Departamento de Ciências Exatas e da Terra, Universidade Federal de São Paulo, CEP 13251-900 Diadema, São Paulo, Brazil; mlente@df.ufscar.br

[1] M. Fiebig, J. Phys. D **38**, 123 (2005).
[2] N. A. Spaldin and M. Fiebig, Science **309**, 391 (2005).
[3] W. Eerenstein, N. D. Mathur, and J. F. Scott, Nat. Mater. **442**, 759 (2006).
[4] H. Schmid, Ferroelectrics **162**, 317 (1994).
[5] M. Fiebig, Th. Lottermoser, D. Frohlich, A. V. Goltsev, and R. V. Pisarev, Nat. Mater. **419**, 818 (2002).
[6] R. E. Newnham and L. E. Cross, Ferroelectrics **10**, 269 (1976).
[7] R. E. Newnham and L. E. Cross, Mater. Res. Bull. **9**, 927 (1974).
[8] L. E. Cross and R. E. Newham, *History of Ferroelectrics*, Ceramics and Civilization Vol. 111 (American Ceramic Society, Columbus, OH, 1987).
[9] L. Cross, Ferroelectrics **76**, 241 (1987).
[10] R. E. Newnham and S. Trolier-McKinstry, Integr. Ferroelectr. **20**, 1 (1998).
[11] H. Schmid, Ferroelectrics **252**, 41 (2001).
[12] D. B. Litvin, V. Janovec, and S. Y. Litvin, Ferroelectrics **162**, 275 (1994).
[13] H. Grimmer, Acta Crystallogr., Sect. A: Found. Crystallogr. **48**, 266 (1992).
[14] A. Filippetti and N. A. Hill, Phys. Rev. B **65**, 195120 (2002).
[15] X. S. Gao, X. Y. Chen, J. Yin, J. Wu, Z. G. Liu, and M. Wang, J. Mater. Sci. **35**, 5421 (2000).
[16] G. Srinivasan, C. P. De Vreugd, V. M. Laletin, N. Paddubnaya, M. I. Bichurin, V. M. Petrov, and D. A. Filippov, Phys. Rev. B **71**, 184423 (2005).

[17] H. Zheng, J. Wang, S. E. Lofland, Z. Ma, L. Mohaddes-Ardabili, T. Zhao, L. Salamanca-Riba, S. R. Shinde, S. B. Ogale, F. Bai, D. Viehland, Y. Jia, D. G. Schlom, M. Wuttig, A. Roytburd, and R. Ramesh, Science **303**, 661 (2004).
[18] J. Ryu, S. Pria, K. Uchino, and H.-EE. Kim, J. Electroceram. **8**, 107 (2002).
[19] R. E. Newnham, Am. Mineral. **59**, 906 (1974).
[20] C.-H. Yang, T. Y. Koo, and Y. H. Jeong, Solid State Commun. **134**, 299 (2005).
[21] G. Catalan, Appl. Phys. Lett. **88**, 102902 (2006).
[22] J. de Los S. Guerra, M. H. Lente, and J. A. Eiras, Appl. Phys. Lett. **88**, 102905 (2006).
[23] M. H. Lente, J. D. S. Guerra, S. Lanfredi, and J. A. Eiras, Solid State Commun. **131**, 279 (2004).
[24] M. H. Lente, J. D. S. Guerra, T. Mazon, M. B. R. Andreeta, A. C. Hernandes, and J. A. Eiras, J. Eur. Ceram. Soc. **25**, 2563 (2005).
[25] J. D. S. Guerra, L. A. Bassora, and J. A. Eiras, Eur. Phys. J.: Appl. Phys. **36**, 65 (2006).
[26] J. D. S. Guerra, L. A. Bássora, and J. A. Eiras, Solid State Commun. **140**, 426 (2006).
[27] S. Ananta and N. W. Thomas, J. Eur. Ceram. Soc. **19**, 1873 (1999).
[28] V. V. Bhat, A. M. Umarji, V. B. Shenoy, and U. V. Waghmare, Phys. Rev. B **72**, 014104 (2005).
[29] S. P. Singh, A. K. Singh, D. Pandey, H. Sarma, and O. Parkash, J. Mater. Res. **18**, 2677 (2003).
[30] V. Bonny, M. Bonin, P. Sciau, K. J. Schenk, and G. Chapuis, Solid State Commun. **102**, 347 (1997).
[31] N. Lampis, P. Sciau, and A. G. Lehmann, J. Phys.: Condens. Matter **11**, 3489 (1999).
[32] S. A. Ivanov, R. Tellgren, H. Rundlof, N. W. Thomas, and S. Ananta, J. Phys.: Condens. Matter **12**, 2393 (2000).
[33] V. A. Vokov, I. E. Mylnikova, and G. A. Smolenskii, Sov. Phys. JETP **15**, 447 (1962).
[34] S. B. Majumder, S. Bhattacharyya, R. S. Katiyar, A. Manivannan, P. Dutta, and M. S. Seehra, J. Appl. Phys. **99**, 024108 (2006).
[35] O. Raymond, R. Font, N. Suárez-Almodovar, J. Portelles, and J. M. Siqueiros, J. Appl. Phys. **97**, 084107 (2005).
[36] R. Blinc, P. Cevc, A. Zorko, J. Holc, M. Kosec, Z. Trontelj, J. Pirnat, N. Dalal, V. Ramachandran, and J. Krzystek, J. Appl. Phys. **101**, 033901 (2007).
[37] Y. Yang, J. M. Liu, H. B. Huang, W. Q. Zou, P. Bao, and Z. G. Liu, Phys. Rev. B **70**, 132101 (2004).
[38] S. Ananta and N. W. Thomas, J. Eur. Ceram. Soc. **19**, 155 (1999).
[39] O. Raymond, R. Font, N. Suárez, J. Portelles, and J. M. Siqueiros, Ferroelectrics **294**, 141 (2003).
[40] M. H. Lente, A. L. Zanin, E. M. Andreeta, D. Garcia, and J. A. Eiras, Appl. Phys. Lett. **85**, 982 (2004).
[41] T. Watanabe and K. Kohn, Phase Transitions **15**, 57 (1989).
[42] S. Lanfredi, M. H. Lente, and J. A. Eiras, Appl. Phys. Lett. **80**, 2731 (2002).
[43] I. Bunget and M. Popescu, *Physics of Solid Dielectrics*, Material Science Monographs Vol. 19 (Elsevier, Amsterdam, 1984), Chap. 5.
[44] J. F. Nye, *Physical Properties of Crystals* (Clarendon, Oxford, 1977).
[45] A. S. Nowick and B. S. Berry, *Anelastic Relaxation in Crystalline Solids* (Academic, London, 1972).
[46] M. S. Seehra and R. E. Helmick, J. Appl. Phys. **55**, 2330 (1984).
[47] J. F. Scott, Phys. Rev. B **16**, 2329 (1977).
[48] M. S. Seehra and R. E. Helmick, Phys. Rev. B **24**, 5098 (1981).
[49] D. F. Gibbons, Phys. Rev. **115**, 1194 (1959).
[50] S. P. Singh, D. Pandey, S. Yoon, S. Baik, and N. Shin, Appl. Phys. Lett. **90**, 242915 (2007).
[51] U. Robels and G. Arlt, J. Appl. Phys. **73**, 3454 (1993).
[52] G. Arlt and N. A. Pertsev, J. Appl. Phys. **70**, 2283 (1991).